Serican Journal of Medicine
2026, VOL. 3, NO. 4, 26309
https://doi.org/10.17161/sjm.v3i4.26309

Identification of a TRPM4-related Gene Signature for Predicting Prognosis, Immune Landscape, and Therapeutic Sensitivity in Bladder Cancer

Pengwei Luo[1*], Haotian Yi[1*], Ruoyuan Ma[2*], Ying Wang[1], Chengyi Wang[1], Pengqiao Wang[1#] and Xi Xie[1#]

[1]Department of Urology, The First Affiliated Hospital of Chengdu Medical College, Chengdu 610500, China
[2]School of Pharmaceutical Sciences, Chengdu Medical College, Chengdu 610500, China

* These authors contributed equally to this work
# Corresponding authors: Xi Xie, MD/PhD, The First Affiliated Hospital of Chengdu Medical College, email:15828379690@163.com; Pengqiao Wang, MD/PhD, The First Affiliated Hospital of Chengdu Medical College, email: 65997304@qq.com

ABSTRACT

Background: Bladder cancer (BLCA) is heterogeneous, and reliable prognostic biomarkers are needed. TRPM4 can mediate sodium-overload necrosis (NECSO), but its relevance to BLCA remains unclear.

Methods: TCGA-BLCA and GEO GSE13507 were used as training and validation cohorts. TRPM4 co-expression, differential-expression, and univariate Cox analyses identified candidate genes. LASSO-Cox regression generated an eight-gene risk score. Pathway enrichment, CIBERSORT, tumor mutational burden (TMB), and pRRophetic analyses characterized its biological and clinical associations.

Results: The eight-gene model separated patients with different survival outcomes in both cohorts. Multivariate analysis supported its independent prognostic value, and a nomogram integrating clinical variables improved prediction. High-risk tumors were enriched in cell-cycle and DNA-replication pathways, whereas low-risk tumors favored metabolic processes and had higher TMB. Estimated M1 macrophage fractions were higher in the high-risk group, while Treg and plasma-cell fractions were higher in the low-risk group. High-risk tumors showed greater predicted sensitivity to cisplatin, gemcitabine, and targeted agents. The M1 finding describes relative immune composition and does not establish stronger functional antitumor activity.

Conclusions: This TRPM4-related signature links prognosis with tumor heterogeneity, immune composition, and predicted drug sensitivity in BLCA. It may support further research into risk stratification and individualized therapy, but its mechanisms and clinical utility require validation.

ARTICLE HISTORY
Received: Oct. 19, 2026
Revised: Nov. 8, 2026
Accepted: Nov. 9, 2026

KEYWORDS
TRPM4, sodium overload necrosis, NECSO, bladder cancer, prognostic model

1. Introduction

Bladder cancer (BLCA) is one of the most common malignancies of the urinary system worldwide. According to GLOBOCAN 2022 statistics, BLCA accounts for approximately 614,300 new cases and 220,600 deaths globally, representing 3.1% and 2.3% of all new cancer cases and cancer deaths worldwide, respectively. It ranks as the sixth most common cancer among men [1]. Clinically, muscle-invasive bladder cancer (MIBC) is treated with radical cystectomy combined with lymph node dissection [2], while non-muscle-invasive bladder cancer (NMIBC) is typically managed by transurethral resection with intravesical instillation therapy [3]. However, due to the high recurrence rate and progression of BLCA, current treatment strategies still offer suboptimal long-term survival outcomes. Therefore, there is an urgent need to identify reliable biomarkers and develop robust prognostic models for personalized precision treatment.

Recent research has increasingly focused on the role of ion channels in tumorigenesis [4, 5]. Transient receptor potential (TRP) channels, which serve as sensors for various signals, are widely expressed in different tissues [6]. Among them, the TRPM subfamily is implicated in multiple pathological processes [7]. TRPM4 is a calcium-activated, non-selective univalent cation channel that, when activated, leads

© 2026 The Author(s). Published by the University of Kansas Libraries.
This is an Open Access article distributed under the terms of the Creative Commons Attribution License (http://creativecommons.org/licenses/by/4.0/)

to massive sodium ion influx, triggering cell membrane depolarization, ATP depletion, mitochondrial dysfunction, and ultimately necrosis through sodium-overload-induced necrosis (NECSO) [8]. TRPM4 has been shown to be overexpressed in several tumors, including breast and prostate cancers, where it regulates cell proliferation and migration [9]. However, its specific role in bladder cancer and its prognostic implications remain unclear.

This study aims to examine TRPM4 expression and its associated gene network in the TCGA-BLCA cohort, construct a prognostic risk model, and explore the biological mechanisms involved. Additionally, we examine the potential application of the TRPM4-mediated NECSO mechanism in personalized therapy for bladder cancer.

Materials and Methods

1. Data acquisition

RNA sequencing (RNA-seq) data (FPKM format), somatic mutation data (MAF format), and associated clinical information for bladder cancer (BLCA) patients were downloaded from The Cancer Genome Atlas (TCGA, https://portal.gdc.cancer.gov/). Transcriptomic and clinical data for the external validation cohort GSE13507 were obtained from the Gene Expression Omnibus (GEO, https://www.ncbi.nlm.nih.gov/geo/). All data originated from public databases and did not require additional ethical review.

2. Identification of TRPM4-related prognostic genes

First, we extracted TRPM4 expression data from the TCGA-BLCA cohort and identified co-expressed genes with TRPM4 via Pearson correlation analysis (selection criteria: $|R| > 0.4$ and $p < 0.001$). Concurrently, we used the R "limma" package to screen for differentially expressed genes (DEGs) between tumor and normal tissues (selection criteria: $|\log2FC| > 1$ and $FDR < 0.05$). The intersection of TRPM4 co-expressed genes and DEGs was further incorporated into univariate Cox regression analysis to identify genes significantly associated with overall survival (OS) ($p < 0.05$), serving as candidate genes for constructing a prognostic model.

3. Construction and validation of the risk scoring model

To prevent model overfitting, candidate genes underwent dimensionality reduction using the Least Absolute Shrinkage and Selection Operator (LASSO) Cox regression algorithm. The optimal penalty parameter (λ) was determined through 10-fold cross-validation, identifying the optimal combination of prognostic genes. The risk score (RiskScore) is calculated as: $\text{RiskScore} = \Sigma(\beta_i \times \text{Expression}_i)$ (where β_i represents the Cox regression coefficient). Patients were stratified into high-risk and low-risk groups based on the median risk score from the TCGA cohort.

4. Functional enrichment analysis

Differentially expressed genes were annotated using Gene Ontology (GO) and subjected to Kyoto Encyclopedia of Genes and Genomes (KEGG) pathway enrichment analysis via the R package "clusterProfiler". Gene Set Enrichment Analysis (GSEA) was performed using the "fgsea" package, with reference gene sets sourced from the MSigDB database. Pathway enrichment significance was determined using thresholds of $p < 0.05$ and $FDR < 0.25$.

5. Immune infiltration and tumor mutation burden (TMB) analysis

This study employed the CIBERSORT algorithm to estimate the immune cell composition within the samples. We obtained FPKM data from the TCGA database, uniformly converted the data to TPM format, then performed $\log_2(\text{TPM}+1)$ transformation for subsequent analysis. The preprocessed matrix was submitted to the CIBERSORT algorithm, using the LM22 feature matrix as reference, to estimate the relative abundance of 22 immune cell subtypes through 1000 permutation tests. To ensure result reliability, we retained only samples with p-values < 0.05 from CIBERSORT outputs and treated negative values as 0. Immunological infiltration differences between high- and low-risk groups were compared using the Wilcoxon signed-rank test, with $p < 0.05$ indicating statistical significance. Spearman correlation analysis was employed to assess the association between model genes, risk scores, and immune cell infiltration. Additionally, the "maftools" package analyzed somatic mutation data to calculate tumor mutational burden (TMB, defined as the total number of non-synonymous mutations per megabase) and generated waterfall plots illustrating mutation pattern differences across risk groups.

6. Drug sensitivity prediction

Based on the Genomic Database of Cancer Sensitivity (GDSC), the half-maximal inhibitory concentration (IC50) for common chemotherapeutic

Figure 1. Co-expression analysis and functional enrichment of TRPM4-related genes in bladder cancer. **A** Co-expression network of TRPM4 in the TCGA-BLCA cohort, showing positively (red) and negatively (blue) correlated genes. **B** Hierarchical clustering tree of Gene Ontology (GO) terms enriched by TRPM4-related genes, with branch colors indicating functional categories. **C** Bubble plot of GO enrichment analysis displaying significantly enriched biological processes, cellular components, and molecular functions. The dimensions of the bubbles are indicative of the number of genes, while the color scale serves to reflect the adjusted p-values. **D** Circular plot of KEGG pathway enrichment analysis, summarizing the number and significance of TRPM4-related prognostic genes involved in different pathways. **E** Bar plot of the top significantly enriched KEGG pathways, including focal adhesion, regulation of actin cytoskeleton, glycerolipid metabolism, sulfur metabolism, and small cell lung cancer. **F** Hierarchical clustering dendrogram of KEGG pathways, highlighting functional modules associated with glycosaminoglycan degradation, fatty acid metabolism, viral infection pathways, and pyruvate metabolism.

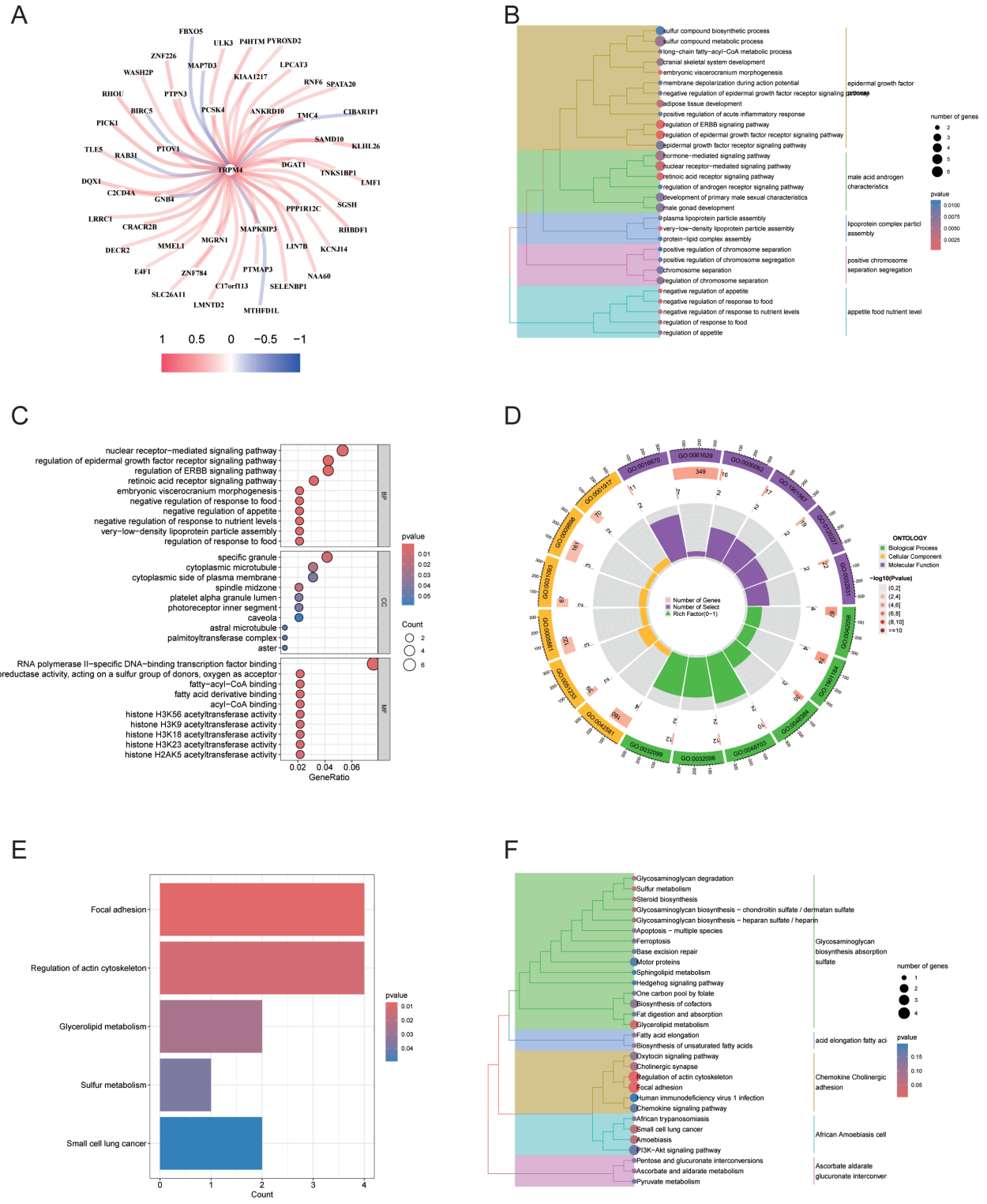

and targeted drugs was predicted using the ridge regression model from the "pRRophetic" package in R. Differences in drug sensitivity between high- and low-risk groups were compared via the Wilcoxon test.

7. Statistical analysis

All statistical analyses were performed using R software (version 4.2.0). Intergroup comparisons of overall survival (OS) and progression-free survival (PFS) were performed using Kaplan-Meier survival curves and the log-rank test. The independent prognostic value of the model was assessed through univariate and multivariate Cox regression analyses. Time-dependent ROC curves were generated using the "timeROC" package to evaluate the predictive performance of the model. $P < 0.05$ (two-tailed) was considered statistically significant.

Results

Identification of TRPM4-related genes and functional enrichment analysis

To explore the molecular regulatory network of TRPM4 in bladder cancer, we first constructed a gene co-expression network centered on TRPM4 using Pearson correlation analysis based on the TCGA-BLCA cohort (Figure 1A). This analysis revealed significant positive correlations ($|R| \geq 0.5$) between TRPM4 and key oncogenes, such as RNF6,TNKS1BP1 and ANKRD10, as well as signaling pathway regulators, suggesting potential interactions in tumorigenesis and progression. Conversely, negative correlations with specific genes point to possible antagonistic regulatory mechanisms. This co-expression network lays the molecular groundwork for identifying key TRPM4-mediated prognostic genes.

Next, Gene Ontology (GO) enrichment analysis identified the biological functions of TRPM4-associated genes across three categories: biological process (BP), cellular component (CC), and molecular function (MF) (Figure 1B-D). At the BP level, these genes were significantly enriched in pathways like ERBB signaling, nuclear receptor-mediated signaling, and lipid metabolism (e.g., plasma lipoprotein assembly, long-chain fatty acid metabolism), suggesting that TRPM4 may promote tumor cell proliferation by reprogramming lipid metabolism and activating oncogenic signaling. At the CC and MF levels, gene products were enriched in the spindle midzone, caveolae, and histone acetyltransferase activity (e.g., modification of H3K9 and H3K18), indicating TRPM4's role in cell division, membrane signaling, and epigenetic regulation.

KEGG pathway analysis further supported these findings (Figure 1E), showing that TRPM4 co-expressed genes were most significantly enriched ($p < 0.01$) in the "Focal adhesion" and "Regulation of actin cytoskeleton" pathways, with the highest gene counts. Additionally, pathways like glycerolipid metabolism and cancer-related pathways (e.g., small cell lung cancer) were also enriched, suggesting common mechanisms across cancers. The pathway clustering heatmap (Figure 1F) revealed that "Focal adhesion" and "Regulation of actin cytoskeleton" formed the closest clusters, with high gene counts and statistical significance. This highlights the synergistic role of the TRPM4 gene network in regulating tumor cell adhesion, cytoskeletal remodeling, and invasive migration.

Together, these findings indicate that TRPM4 and its co-expressed genes are crucial in bladder cancer pathogenesis, involving processes such as cell cycle regulation, metabolic reprogramming, and cytoskeletal dynamics.

Construction and validation of the prognostic risk model

First, univariate Cox regression analysis identified 20 TRPM4-associated genes significantly correlated with overall survival (OS) in the TCGA-BLCA cohort (Figure 2A). Among these, genes such as GNB4, TNKS1BP1, DNAJC11, LAMA4, ACTN4, and FAM126A had hazard ratios (HR) > 1, indicating they are risk factors, while genes like SELENBP1, SPATA20, ANKRD10, and STXBP2 had HR < 1, suggesting protective roles. To enhance model robustness and prevent overfitting, LASSO-Cox regression analysis was used for dimensionality reduction of candidate genes (Figure 2B). The optimal penalty parameter (λ) was determined via 10-fold cross-validation, which led to the selection of eight key genes—SELENBP1, TNKS1BP1, ANKRD10, FAM126A, STXBP2, DNAJC11, LAMA4, and ACTN4—for the risk score model (Figure 2C). The risk score (RiskScore) is calculated as follows:

$$\begin{aligned}\text{RiskScore} = {} & -0.1803 \times \text{SELENBP1} + 0.4015 \times \text{TNKS1BP1} - 0.3945 \times \text{ANKRD10} \\ & + 0.4849 \times \text{FAM126A} - 0.7487 \times \text{STXBP2} + 0.5128 \times \text{DNAJC11} \\ & + 0.3286 \times \text{LAMA4} + 0.4141 \times \text{ACTN4}\end{aligned}$$

Figure 2. Construction and validation of the prognostic risk model based on TRPM4-related genes. **A** The forest plot of the univariate Cox regression analysis identifies prognostic genes in the TCGA-BLCA cohort. Genes with hazard ratios (HR) greater than 1.0 were designated as risk factors, whereas those with HR less than 1.0 were classified as protective factors. **B** The objective of LASSO regression with 10-fold cross-validation is to identify the optimal penalty parameter (λ) by minimizing the partial likelihood deviance. **C** The LASSO coefficient profiles of candidate prognostic genes across a range of log(λ) values were utilized to select eight genes for model construction. **D** Kaplan-Meier survival analysis comparing overall survival (OS) between high-risk and low-risk groups in the TCGA cohort. **E** The external validation of the risk model in the GEO cohort (GSE13507) entailed a comparison of overall survival (OS) between high-risk and low-risk groups. **F** Kaplan-Meier analysis comparing progression-free survival (PFS) between high-risk and low-risk groups in the TCGA cohort.

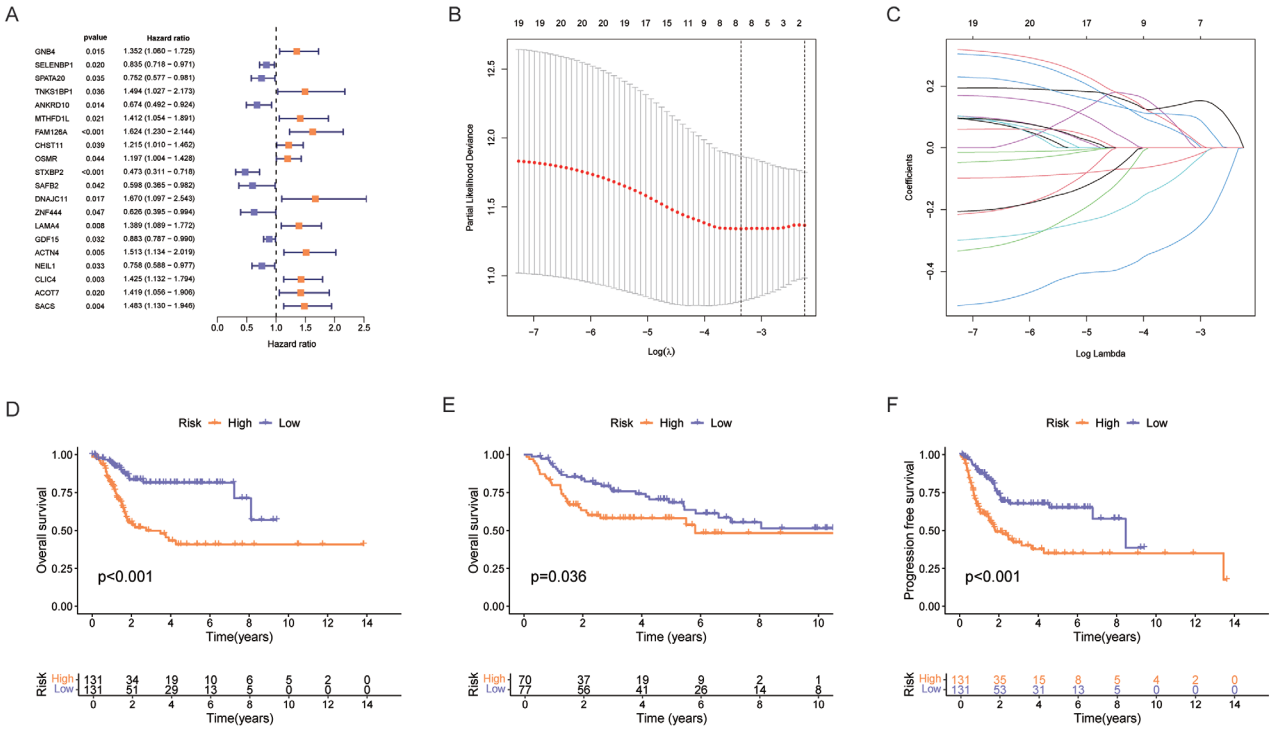

Using this formula, we calculated the risk score for each patient in the TCGA training cohort. The median method was then used to determine the optimal cutoff value (cutoff) by maximizing the survival difference between high- and low-risk groups. This cutoff was the median risk score, dividing the cohort into high- and low-risk groups accordingly.

Kaplan-Meier survival analysis showed significantly lower overall survival in the high-risk group compared to the low-risk group in the TCGA training cohort ($p < 0.001$, Figure 2D), indicating a strong association between higher risk scores and poor prognosis. For external validation, we applied the model formula and cutoff value from the TCGA training cohort to the GEO external validation cohort (GEO: GSE13507). Using gene expression data from the GEO cohort, we calculated risk scores and grouped patients based on the same cutoff. The results confirmed that survival rates were significantly lower in the high-risk group ($p = 0.036$, Figure 2E), demonstrating the model's strong generalizability. Furthermore, in progression-free survival (PFS) analysis, high-risk patients showed faster disease progression and shorter PFS ($p < 0.001$, Figure 2F).

These findings collectively highlight that the eight-gene risk score model is highly accurate and stable in predicting the prognosis of bladder cancer patients.

Independent prognostic value and predictive performance of the risk model

To evaluate whether the risk score acts as an independent prognostic indicator beyond traditional clinical and pathological factors, we conducted both univariate and multivariate Cox regression analyses. The univariate analysis showed that age, clinical stage, N stage, and risk score were significantly associated with overall survival (OS) ($p < 0.001$, Figure 3A). Further multivariate Cox regression analysis

Figure 3: Independent prognostic value and predictive performance of the eight-gene risk model in bladder cancer. **A & B** Univariate (A) and Multivariate (B) Cox Regression Analysis of Clinical Variables and Risk Scores in the TCGA-BLCA Cohort. **C** ROC curves are employed to compare the predictive performance of the risk score with that of traditional clinical parameters. **D** The distribution of risk scores and survival status plots for patients is presented. **E** The temporal variation of the risk model's time-dependent ROC curves is demonstrated for 1-, 3-, and 5-year overall survival outcomes. **F** The heatmap illustrates the expression patterns of the eight model genes in both high- and low-risk groups.

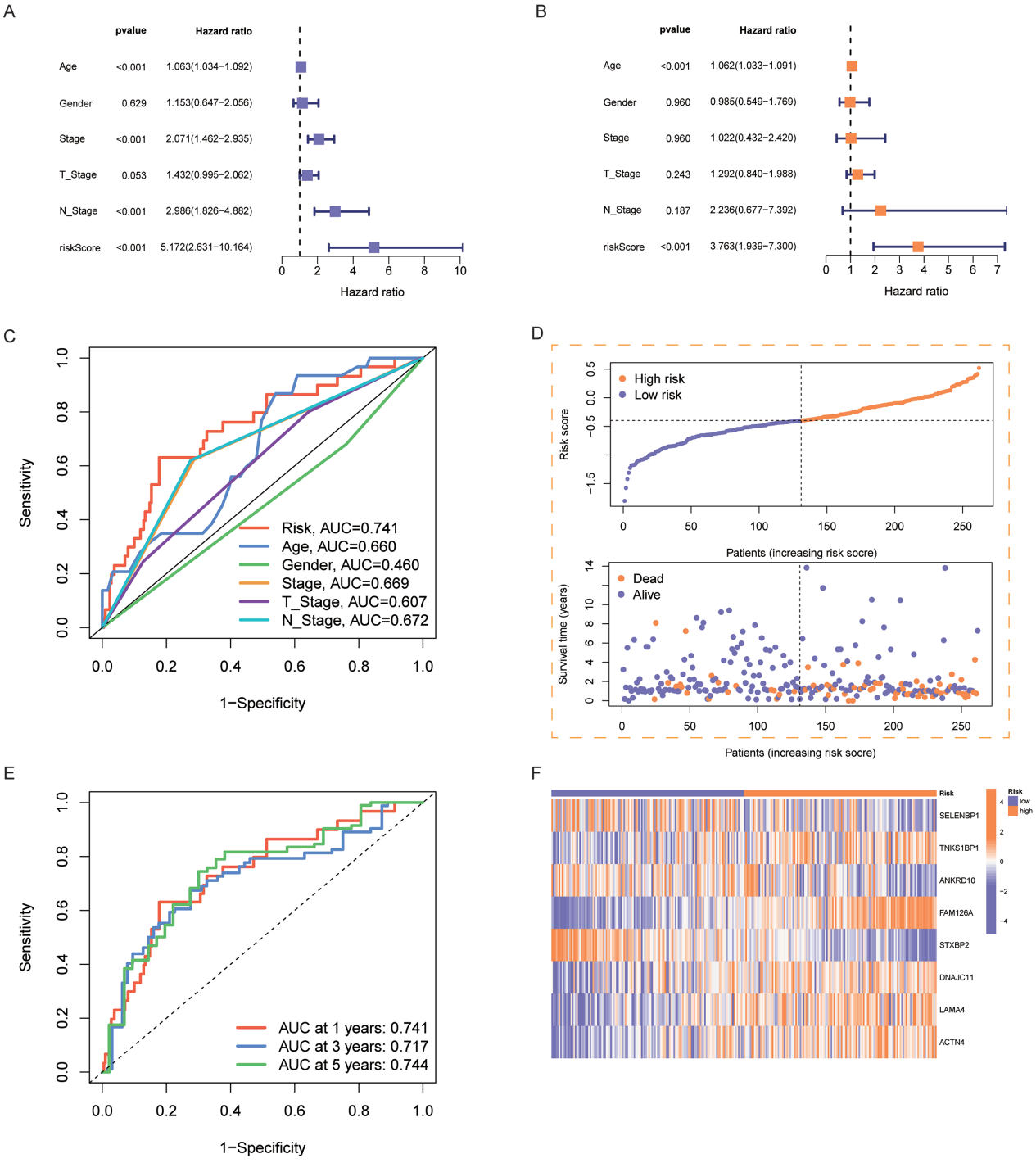

Figure 4. Nomogram construction and stratified survival analysis of the risk model combined with clinical features in bladder cancer. **A** Nomogram integrating M stage, gender, clinical stage, age, N stage, T stage, and risk score for predicting 1-, 3-, and 5-year overall survival (OS) in patients with bladder cancer. **B** The OS calibration curve demonstrates a high degree of consistency between predicted and observed 1-year, 3-year, and 5-year survival probabilities. **C - G** Stratified Kaplan-Meier survival analysis of risk scores was conducted across a range of clinical subgroups: gender (C), age (≤65 *vs*. >65 years) (D), clinical stage (Stage I–II *vs*. Stage III–IV) (E), T stage (T1–2 *vs*. T3–4) (F), and N stage (N0 *vs*. N1) (G).

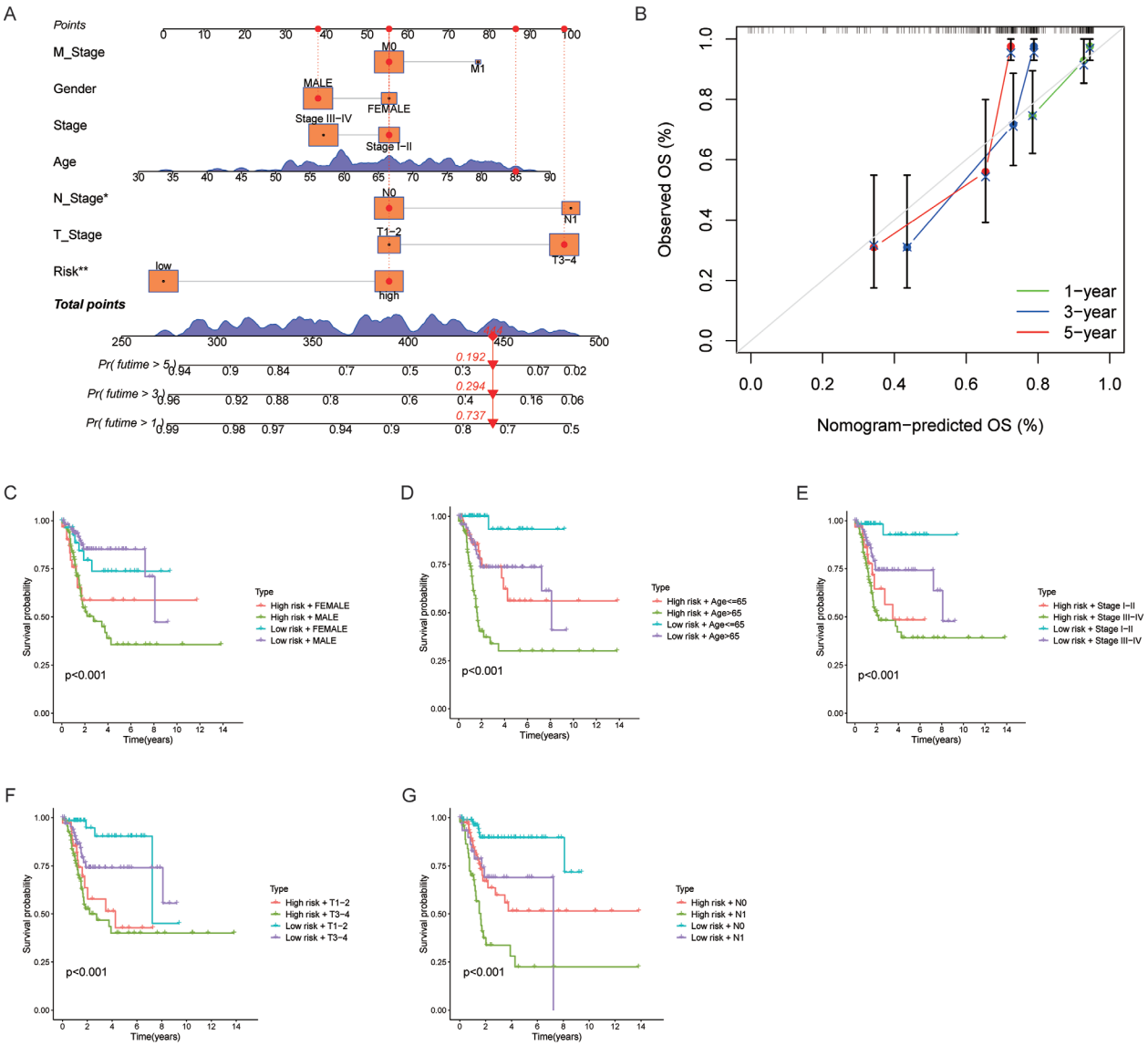

confirmed that the risk score remained a significant independent factor for OS, even after adjusting for confounding variables such as gender, age, and clinical stage and T/N staging (HR > 1, p < 0.001, Figure 3B). Age also demonstrated independent prognostic value.

We then assessed the predictive performance of the model using a ROC curve (Figure 3C). The area under the curve (AUC) for the risk score was 0.741, outperforming traditional clinical parameters like age, gender, clinical stage, and T/N stage, indicating superior predictive accuracy. Time-dependent ROC analysis revealed AUC values of 0.741, 0.717, and 0.744 for predicting 1-, 3-, and 5-year survival rates, respectively (Figure 3E), showing stable performance over time.

The risk distribution and survival status plot (Figure 3D) visually demonstrated the relationship between risk scores and patient prognosis: as risk scores increased, mortality events significantly rose and survival time decreased. The gene heatmap (Figure 3F) further validated the expression patterns

Figure 5. Functional enrichment, tumor mutation burden, and immune infiltration analysis between high- and low-risk groups. **A** Gene set enrichment analysis (GSEA). **B** The landscape of somatic mutations in the TCGA-BLCA cohort has been stratified by risk score. **C** A comparative analysis of immune cell infiltration has been conducted between high- and low-risk groups, employing the CIBERSORT algorithm as an analytical framework. **D** Heatmap showing the correlations between the expression of model genes, risk score, and immune cell infiltration.

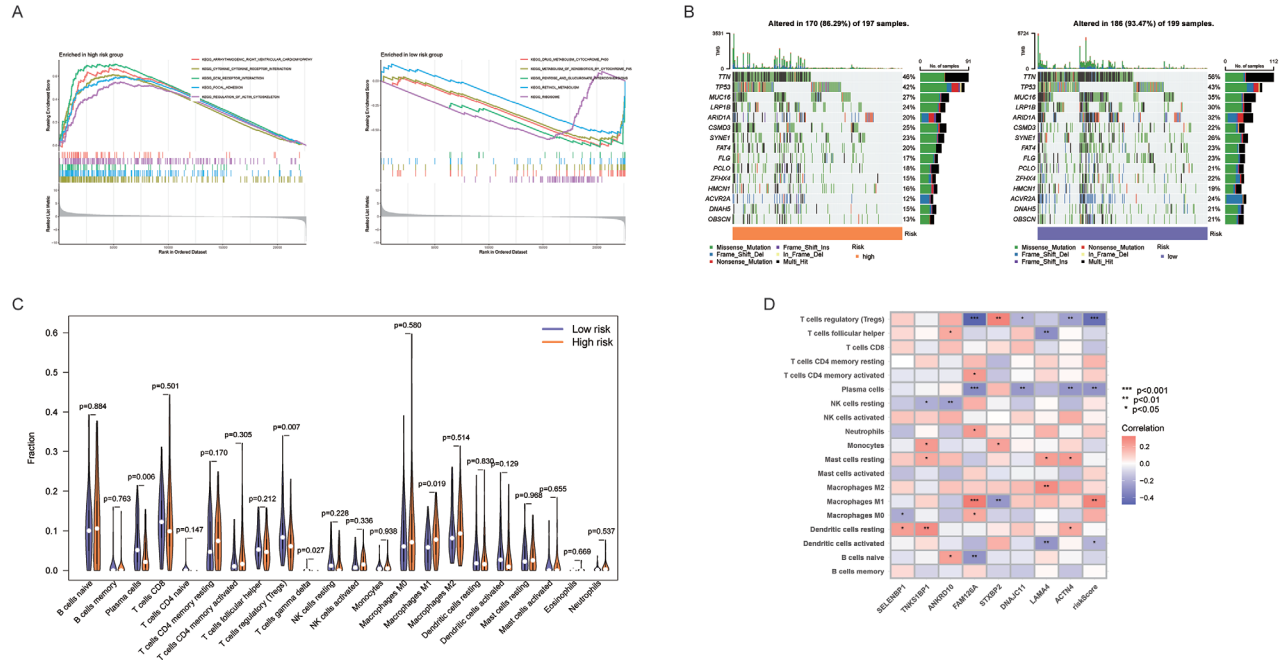

of model genes, showing that high-risk genes like FAM126A, DNAJC11, and LAMA4 were significantly overexpressed in the high-risk group, while protective genes were under-expressed. Collectively, these results indicate that the eight-gene risk score model is a stable, independent, and highly effective prognostic tool.

Construction of a nomogram and subgroup survival analysis

To improve the clinical utility of the risk scoring model, we combined the risk group with traditional clinical characteristics, including age, gender, clinical stage, and T/N/M staging, to construct a nomogram that predicts 1-year, 3-year, and 5-year overall survival (OS) in bladder cancer patients (Figure 4A). Calibration curve analysis showed strong agreement between the predicted survival probabilities from the nomogram and the observed survival rates at 1, 3, and 5 years (Figure 4B). The curves closely followed the diagonal line, confirming the nomogram's accuracy and reliability in predicting individualized patient prognosis.

We further evaluated the model's generalizability across various clinical subgroups using Kaplan-Meier survival analysis (Figures 4C-G). The results showed that, in all subgroups stratified by age (≤65 vs. >65 years), sex, clinical stage (I–II vs. III–IV), T stage (T1-2 vs. T3-4), and N stage (N0 vs. N1), patients in the high-risk group had significantly worse overall survival compared to those in the low-risk group ($p < 0.05$). These findings demonstrate that the eight-gene risk score model provides strong prognostic discrimination, unaffected by clinical-pathological heterogeneity, and is applicable to a wide patient population.

Functional enrichment, mutation landscape, and immune infiltration characteristics

Gene Set Enrichment Analysis (GSEA) identified potential biological mechanisms associated with different risk groups (Figure 5A). The high-risk group was significantly enriched in pathways related to cell proliferation and invasion, including cytokine-cytokine receptor interactions, ECM-receptor interactions, focal adhesions, and actin cytoskeleton regulation. In contrast, the low-risk group showed enrichment in metabolic processes such as retinol metabolism, drug metabolism (cytochrome P450), andpentose and glucuronate interconversion pathways. These results suggest that the poor prognosis in the high-risk group may be linked to

active cell proliferation and extracellular matrix remodeling, while the low-risk group retains more active metabolic functions.

To explore the relationship between genomic features and risk stratification, we performed somatic mutation analysis and assessed tumor mutational burden (TMB) in the TCGA-BLCA cohort (Figure 5B). The low-risk group had significantly higher mutation coverage (93.47%) compared to the high-risk group (86.29%). Regarding TMB, the low-risk group exhibited greater genomic instability, with a maximum TMB value of 5724, compared to 3531 in the high-risk group. Although TTN, TP53, and MUC16 were the most frequently mutated genes in both groups, their mutation profiles differed significantly: TTN mutations occurred more frequently in the low-risk group (56%) compared to the high-risk group (46%). TP53 mutations were similarly frequent in both groups (43% vs. 42%), suggesting that TP53 alterations are a common event in bladder cancer progression. Other key genes such as MUC16 (35% vs. 27%), ARID1A (32% vs. 20%), and LRP1B (30% vs. 24%) had higher mutation frequencies in the low-risk group. Additionally, the proportion of Multi_Hit (multiple mutations) was higher in the low-risk group for several prospective driver genes (e.g., TTN, MUC16, ARID1A).

Immune cell infiltration analysis revealed significant differences in the tumor microenvironment (TME) (Figure 5C). The low-risk group showed increased infiltration of regulatory T cells (Tregs), γδ T cells, and plasma cells ($p < 0.05$), suggesting an immunosuppressive environment. In contrast, the high-risk group exhibited a significant enrichment of M1 macrophages, a finding that reflects estimated cell composition rather than direct evidence of stronger functional antitumor activity. Spearman correlation analysis (Figure 5D) confirmed significant associations between model genes such as FAM126A and STXBP2, risk scores, and the abundance of these immune cells, indicating that this eight-gene model accurately reflects the immune phenotype of the bladder cancer microenvironment.

Drug sensitivity prediction

To explore the potential of risk scoring models in guiding clinical drug use, we applied the pRRophetic algorithm using transcriptome data to predict the sensitivity of patients in different risk groups to chemotherapy and targeted drugs (quantified by IC_{50} values, Figures 6A-6X). The results showed significantly lower IC_{50} values in high-risk patients for cisplatin and several targeted agents (dasatinib, olaparib, osimertinib), indicating increased sensitivity and potential therapeutic benefit for this group. In contrast, the low-risk group demonstrated higher predicted resistance to these drugs. In conclusion, this risk scoring model not only effectively stratifies prognosis but also serves as a tool for predicting drug efficacy, supporting the development of more targeted and personalized treatment strategies for high-risk patients.

Discussion

Disruption of ionic homeostasis within the tumor microenvironment (TME) is a key factor driving malignant tumor progression. Changes in sodium ion concentration significantly impact cellular osmotic pressure, metabolic reprogramming, and immune surveillance functions [10]. TRPM4, a calcium-activated, non-selective cation channel, induces a large sodium influx upon sustained activation. This results in cell membrane depolarization, ATP depletion, and osmotic swelling, ultimately leading to NECSO [11-15]. Although TRPM4 has been linked to the development of several solid tumors [16], its role in mediating NECSO and its prognostic value and clinical significance in bladder cancer (BLCA) remain unclear. This study presents the first eight-gene prognostic risk model based on TRPM4-associated co-expression networks, systematically exploring its potential for assessing patient prognosis, understanding the immune microenvironment, and guiding personalized therapy.

A key finding of this study is that the risk model based on TRPM4-related genes strongly correlates with the genomic alteration landscape of bladder cancer (BLCA). Notably, patients in the low-risk group exhibited significantly higher tumor mutational burden (TMB) and increased gene mutation frequencies (e.g., TTN 56%, MUC16 35%), which presents a biologically coherent contradiction to their favorable prognosis. In an immunological context, high TMB typically indicates a greater abundance of neoantigens within tumor tissues. These abnormal proteins are effectively recognized by the host immune system, triggering robust anti-tumor immune responses [17]. However, the CIBERSORT results showed a higher estimated fraction of M1 macrophages in the high-risk group, rather than the low-risk group. The mutation findings therefore do not by themselves explain the observed direction of M1 macrophage enrichment.

Figure 6. An analysis of chemotherapeutic and targeted drug sensitivity is conducted in the context of a risk model for bladder cancer. A-X Box plot displays estimated half-maximal inhibitory concentrations (IC_{50}) for multiple chemotherapy agents and targeted therapies, predicted by the pRRophetic algorithm for high-risk versus low-risk groups.

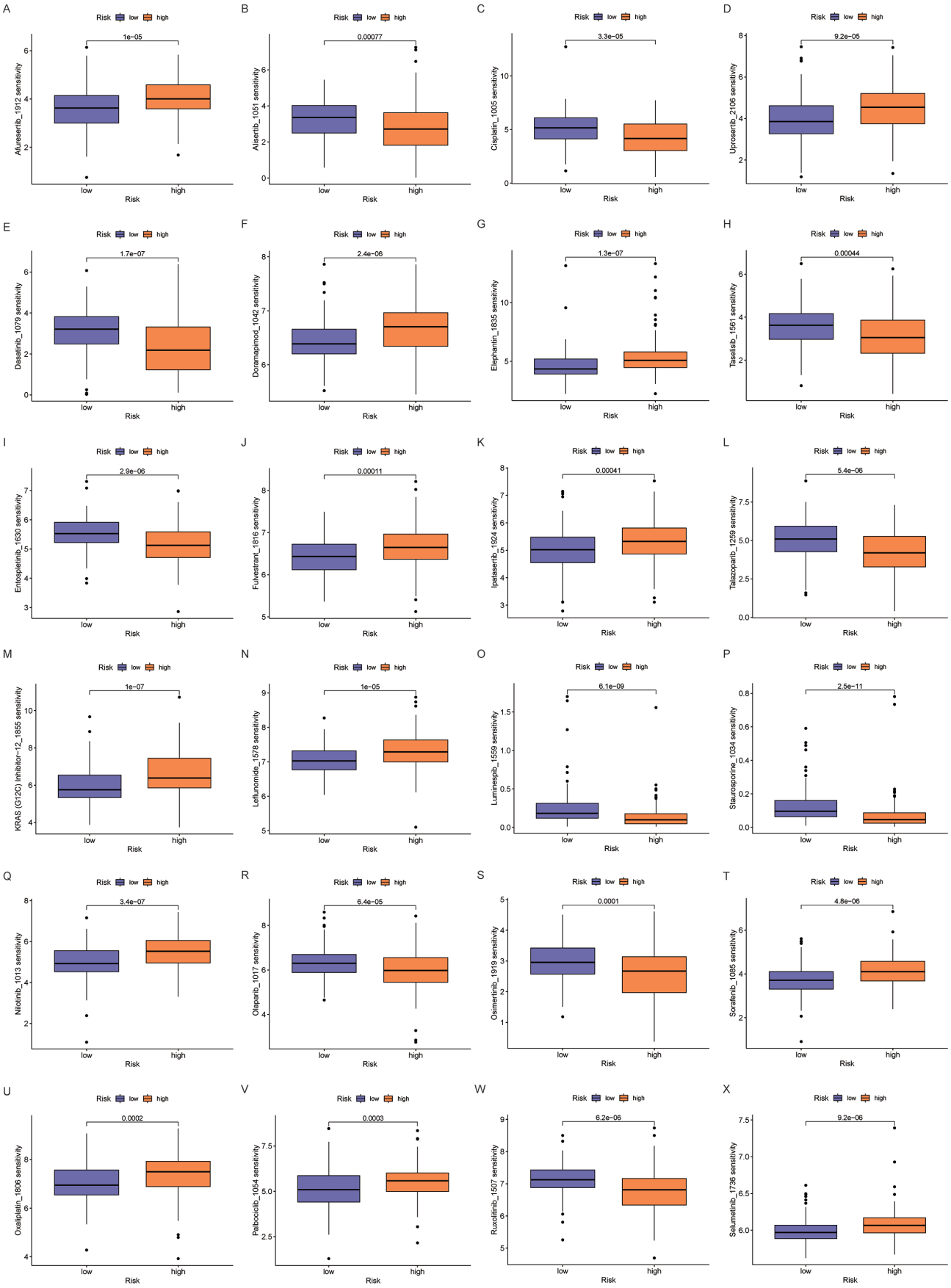

In contrast, the high-risk group exhibits a "low mutation burden but high malignancy" profile. Despite a lower TMB, this group shows significant enrichment in pathways related to "adhesion foci" and "actin cytoskeleton regulation" at the cellular level. This suggests that tumor evolution in the high-risk group may rely more on TRPM4-mediated cytoskeletal remodeling and alterations in the local ionic microenvironment, rather than extensive genomic damage. We further propose a "necrosis-induced immunosuppression" hypothesis: sustained TRPM4 activation in the high-risk group may lead to chronic sodium overload necrosis (NECSO), with continuously released damage-associated molecular patterns (DAMPs) promoting a chronic inflammatory microenvironment [18]. However, the estimated fractions of regulatory T cells (Tregs) and plasma cells were higher in the low-risk group, so their preferential recruitment to the high-risk group is not supported by Figure 5C.

Despite the poorer prognosis of high-risk group patients, drug sensitivity analysis revealed a clinically transformative finding: this group exhibits heightened sensitivity to first-line bladder cancer chemotherapies such as cisplatin and gemcitabine, as well as targeted agents like dasatinib. This aligns with the "high proliferation, high sensitivity" principle of tumor biology: high-risk tumors, enriched in ECM-receptor interaction and characterized by rapid cell division, may respond more strongly to chemotherapy drugs that target rapidly proliferating cells. This insight provides crucial guidance for precision treatment in bladder cancer: although high-risk patients have a more aggressive disease course, they may benefit most from neoadjuvant chemotherapy (NAC) or adjuvant chemotherapy post-surgery. Aggressive systemic treatment may significantly improve their outcomes [19-21]. In contrast, low-risk patients, with slow tumor proliferation, active metabolism, and low predicted chemotherapy sensitivity, may be better suited for surgical resection or bladder-sparing therapies [2]. Over-treatment with chemotherapy should be avoided to minimize toxicity.

Additionally, the eight-gene risk scoring model, developed using Cox and Lasso algorithms, demonstrated robust predictive performance in both the TCGA and GEO cohorts. Compared to traditional TNM staging, this risk score was validated as an independent prognostic indicator, and the combined nomogram significantly improved survival prediction accuracy. This suggests that integrating molecular features (NECSO-associated genes) with clinical-pathological characteristics enables more precise identification of high-risk patients, compensating for the limitations of traditional clinical staging.

Although M1-like macrophages are generally associated with pro-inflammatory and antitumor functions, their enrichment in a high-risk group does not necessarily imply improved survival. In muscle-invasive bladder cancer, combined evaluation of macrophage infiltration and polarization has identified distinct immune environments and clinical outcomes, indicating that abundance should be interpreted together with the wider tumor context [22]. In our study, the high-risk group was defined by an eight-gene prognostic score; it was not defined by macrophage abundance. The observed enrichment therefore does not demonstrate that M1 macrophages independently predict poor survival or cause tumor progression.

Macrophage activation is heterogeneous and depends on cellular origin, local stimuli, and the markers used to define an activation state. The M1/M2 framework does not capture all activation programs present in vivo [23]. Thus, a transcriptomic M1-like classification does not establish that these cells retain effective antigen-presentation or tumoricidal functions within an individual tumor. One possible explanation is that inflammatory-cell recruitment represents a response to aggressive tumor biology that is insufficient to overcome other tumor-promoting processes. This remains a hypothesis, because macrophage function, spatial localization, and the relevant interactions were not directly measured.

Methodological considerations also limit this interpretation. CIBERSORT estimates reference-based relative fractions from bulk expression profiles rather than directly measuring absolute cell density or functional activity [24]. Changes in the proportions of other immune populations can therefore affect the estimated M1 fraction. Higher M1 estimates may coexist with adverse clinical features or other immune-regulatory processes, and a between-group comparison does not resolve these relationships. Consequently, our findings should be interpreted as an association between the multigene risk signature and immune composition, rather than evidence that the established antitumor role of M1 macrophages has been reversed. Independent analyses of macrophage-associated survival effects, together with spatial, single-cell, and functional validation, are needed.

However, this study has several limitations. First, it primarily relies on retrospective analysis of public databases. While validated by external cohorts, the findings require confirmation from multicenter prospective clinical data. Second, although the established model shows good performance in patient prognosis stratification, its potential clinical utility as a drug efficacy predictor requires validation through experimental and clinical trials. Furthermore, the molecular mechanisms by which TRPM4-mediated NECSO specifically recruits Tregs and influences cytoskeletal remodeling warrant further investigation in vitro and in vivo.

In summary, this study elucidates how TRPM4-associated genes influence bladder cancer prognosis by regulating extracellular matrix interactions, cytoskeletal remodeling, and the immune microenvironment. It also reveals the clinical characteristic of "poor prognosis but chemotherapy sensitivity" in high-risk patients. The eight-gene model holds promise as an effective clinical tool for risk stratification and the development of personalized precision treatment strategies for bladder cancer.

Conclusion

This study developed an innovative eight-gene risk scoring model based on TRPM4, a key regulator of NECSO. The model demonstrated strong independent prognostic value across a multicenter cohort. Mechanistic analyses show that high-risk scores are closely linked to genomic instability, cytoskeletal remodeling, and immunosuppressive microenvironments, which explain the biological basis for increased invasiveness and poor prognosis. Clinically, this study highlights that although patients in the high-risk group have shorter survival, they are significantly more sensitive to first-line chemotherapies like cisplatin and gemcitabine, as well as certain targeted therapies. In conclusion, this model not only enhances our understanding of TRPM4's role in bladder cancer but also provides solid theoretical support and practical guidance for identifying high-risk patients and developing precision neoadjuvant chemotherapy or targeted therapy strategies.

Data Availability Statement

The datasets analyzed in this study are publicly available. The TCGA-BLCA dataset was retrieved from The Cancer Genome Atlas (https://portal.gdc.cancer.gov/), and the external validation dataset was obtained from the Gene Expression Omnibus (GEO, https://www.ncbi.nlm.nih.gov/geo/) under accession number GSE13507. All relevant codes and processed data supporting the conclusions of this article are available from the corresponding author upon reasonable request.

Conflict of Interest Statement

The authors declare that the research was conducted in the absence of any commercial or financial relationships that could be construed as a potential conflict of interest.

Ethical Approval

This study utilized publicly available, de-identified patient data from TCGA and GEO. Therefore, ethical approval and informed consent were not required in accordance with local legislation and institutional guidelines.

Acknowledgements

This work was supported by the Foundation of Health Commission of Chengdu (Grant No. 2022071) and the Research Fund of Chengdu Medical College (Grant No. CYZYB25-05).

Author Contribution

Study design: Peng-Wei L and Xi X; Experiments and data analysis: Peng-Wei L, Ruo-Yuan M, Peng-Qiao W, Ying W, Cheng-Yi W, Hao-Tian Y and Xi X; Manuscript draft: Peng-Wei L and Ruo-Yuan M; Manuscript revision: All authors.

References

1. Bray F, Laversanne M, Sung H, Ferlay J, Siegel RL, Soerjomataram I, Jemal A: **Global cancer statistics 2022: GLOBOCAN estimates of incidence and mortality worldwide for 36 cancers in 185 countries**. *CA Cancer J Clin* 2024, **74**(3):229–263; doi:10.3322/caac.21834.
2. Teoh JY, Kamat AM, Black PC, Grivas P, Shariat SF, Babjuk M: **Recurrence mechanisms of non-muscle-invasive bladder cancer - a clinical perspective**. *Nat Rev Urol* 2022, **19**(5):280–294; doi:10.1038/s41585-022-00578-1.
3. Lopez-Beltran A, Cookson MS, Guercio BJ, Cheng L: **Advances in diagnosis and treatment of bladder cancer**. *BMJ* 2024, **384**:e076743; doi:10.1136/bmj-2023-076743.
4. Li L, Chen C, Chiang C, Xiao T, Chen Y, Zhao

Y, Zheng D: **The Impact of TRPV1 on Cancer Pathogenesis and Therapy: A Systematic Review**. *Int J Biol Sci* 2021, **17**(8):2034–2049; doi:10.7150/ijbs.59918; PMC8193258.

5. Wojtera B, Ostrowska K, Szewczyk M, Masternak MM, Golusinski W: **Chloride intracellular channels in oncology as potential novel biomarkers and personalized therapy targets: a systematic review**. *Rep Pract Oncol Radiother.* 2024; **29**(2):258–270; doi:10.5603/rpor.99674; PMC11321771.
6. Zhang M, Ma Y, Ye X, Zhang N, Pan L, Wang B: **TRP (transient receptor potential) ion channel family: structures, biological functions and therapeutic interventions for diseases**. *Signal Transduct Target Ther* 2023, **8**(1):261; doi:10.1038/s41392-023-01464-x; PMC10319900.
7. Jimenez I, Prado Y, Marchant F, Otero C, Eltit F, Cabello-Verrugio C, Cerda O, Simon F: **TRPM Channels in Human Diseases**. *Cells* 2020, **9**(12):2604; doi:10.3390/cells9122604; PMC7761947.
8. Fu W, Wang J, Li T, Qiao Y, Zhang Z, Zhang X, He M, Su Y, Zhao Z, Li C, *et al.*: **Persistent activation of TRPM4 triggers necrotic cell death characterized by sodium overload**. *Nat Chem Biol* 2025, **21**(8):1238–1249; doi:10.1038/s41589-025-01841-3.
9. Borgstrom A, Peinelt C, Stoklosa P: **TRPM4 in Cancer-A New Potential Drug Target**. *Biomolecules* 2021, **11**(2):229; doi:10.3390/biom11020229; PMC7914809.
10. Leslie TK, James AD, Zaccagna F, Grist JT, Deen S, Kennerley A, Riemer F, Kaggie JD, Gallagher FA, Gilbert FJ *et al.*: **Sodium homeostasis in the tumour microenvironment**. *Biochim Biophys Acta Rev Cancer* 2019, **1872**(2):188304; doi:10.1016/j.bbcan.2019.07.001; PMC7115894.
11. Vennekens R, Nilius B: **Insights into TRPM4 function, regulation and physiological role**. *Handb Exp Pharmacol* 2007(179):269–285; doi:10.1007/978-3-540-34891-7_16.
12. Launay P, Fleig A, Perraud AL, Scharenberg AM, Penner R, Kinet JP: **TRPM4 is a Ca2+-activated nonselective cation channel mediating cell membrane depolarization**. *Cell* 2002, **109**(3):397–407; doi:10.1016/s0092-8674(02)00719-5.
13. Dai Y, Wang H, Wang W, Zhuang X: **Multidimensional pan-cancer analysis of the sodium-induced cell death gene TRPM4**. *Sci Rep* 2025, **15**(1):29768; doi:10.1038/s41598-025-15082-w; PMC12350802.
14. Earley S, Waldron BJ, Brayden JE: **Critical role for transient receptor potential channel TRPM4 in myogenic constriction of cerebral arteries**. *Circ Res* 2004, **95**(9):922–929; doi:10.1161/01.RES.0000147311.54833.03.
15. Barbet G, Demion M, Moura IC, Serafini N, Leger T, Vrtovsnik F, Monteiro RC, Guinamard R, Kinet JP, Launay P: **The calcium-activated nonselective cation channel TRPM4 is essential for the migration but not the maturation of dendritic cells**. *Nat Immunol* 2008, **9**(10):1148–1156; doi:10.1038/ni.1648; PMC2956271.
16. Gao Y, Liao P: **TRPM4 channel and cancer**. *Cancer Lett* 2019, **454**:66–69; doi:10.1016/j.canlet.2019.04.012.
17. Sun S, Liu L, Zhang J, Sun L, Shu W, Yang Z, Yao H, Zhang Z: **The role of neoantigens and tumor mutational burden in cancer immunotherapy: advances, mechanisms, and perspectives**. *J Hematol Oncol* 2025, **18**(1):84; doi:10.1186/s13045-025-01732-z; PMC12406617.
18. Chen F, Tang H, Cai X, Lin J, Kang R, Tang D, Liu J: **DAMPs in immunosenescence and cancer**. *Semin Cancer Biol* 2024, **106-107**:123–142; doi:10.1016/j.semcancer.2024.09.005.
19. Gouin KH, 3rd, Ing N, Plummer JT, Rosser CJ, Ben Cheikh B, Oh C, Chen SS, Chan KS, Furuya H, Tourtellotte WG *et al.*: **An N-Cadherin 2 expressing epithelial cell subpopulation predicts response to surgery, chemotherapy and immunotherapy in bladder cancer**. *Nat Commun* 2021, **12**(1):4906; doi:10.1038/s41467-021-25103-7; PMC8361097.
20. Morton D, Seymour M, Magill L, Handley K, Glasbey J, Glimelius B, Palmer A, Seligmann J, Laurberg S, Murakami K, *et al.*: **Preoperative Chemotherapy for Operable Colon Cancer: Mature Results of an International Randomized Controlled Trial**. *J Clin Oncol* 2023, **41**(8):1541–1552; doi:10.1200/JCO.22.00046; PMC10022855.
21. Tanaka R, Endo S, Yamaguchi T, Miyagaki H, Kawada J, Omori T, Takahashi N, Masuzawa T, Furukawa H, Sato Y, *et al.*: **Neoadjuvant docetaxel, oxaliplatin, and S-1 therapy for patients with large type 3 or type 4 gastric cancer: short-term outcomes of a multicenter, phase II study (OGSG1902)**. *Gastric Cancer* 2025, **28**(4):662–672; doi:10.1007/s10120-025-01608-8.

22. Sun M, Zeng H, Jin K, Liu Z, Hu B, Liu C, Yan S, Yu Y, You R, Zhang H *et al.*: **Infiltration and Polarization of Tumor-associated Macrophages Predict Prognosis and Therapeutic Benefit in Muscle-Invasive Bladder Cancer**. *Cancer Immunol Immunother* 2022, **71**(6):1497–1506; doi:10.1007/s00262-021-03098-w; PMC10991313.
23. Murray PJ, Allen JE, Biswas SK, Fisher EA, Gilroy DW, Goerdt S, Gordon S, Hamilton JA, Ivashkiv LB, Lawrence T, *et al.*: **Macrophage activation and polarization: nomenclature and experimental guidelines**. *Immunity* 2014, **41**(1):14–20; doi:10.1016/j.immuni.2014.06.008; PMC4123412.
24. Newman AM, Liu CL, Green MR, Gentles AJ, Feng W, Xu Y, Hoang CD, Diehn M, Alizadeh AA: **Robust enumeration of cell subsets from tissue expression profiles**. *Nat Methods* 2015, **12**(5):453–457; doi:10.1038/nmeth.3337; PMC4739640.